

Molecular orientation in uniaxially drawn poly(aryl ether ether ketone): 2. Infra-red spectroscopic study

A. M. Voice, D. I. Bower* and I. M. Ward

IRC in Polymer Science and Technology, Department of Physics,
The University of Leeds, Leeds LS2 9JT, UK

(Received 6 April 1992)

The development of orientation has been studied in samples of poly(aryl ether ether ketone) (PEEK) drawn at 150°C from initially amorphous material of thickness 7 μm at an initial strain rate of 40% min^{-1} to draw ratios λ in the range 1–2.92. A sample of increased crystallinity and orientation was produced by annealing a sample with $\lambda = 2.92$ at 300°C. Polarized spectra were obtained in the range 640–2000 cm^{-1} . By suitably combining parallel and perpendicular spectra it was possible to predict the spectra of randomly oriented samples with different crystallinities. The conclusion of Nguyen and Ishida that the spectrum of PEEK may be regarded as the sum of two overlapping spectra, due to molecules in amorphous and crystalline conformations, was then confirmed both by spectral subtraction and by curve fitting and shown to account for the apparent shift of peaks with change of polarization direction for oriented samples. The areas under the characteristic peaks have been used to show that the content of crystalline conformers exceeds the degree of crystallinity except for the most highly oriented sample and the annealed sample, and an explanation has been found for the observation of Chalmers *et al.* that there is a linear relationship between the ratio of the absorbances at 1306 and 1280 cm^{-1} and the degree of crystallinity. The C=O stretching mode has been used to derive the orientation average $\langle P_2(\cos \theta) \rangle_c$ for the molecules in the crystalline conformation and this is found to be very much lower than that of the chains in the crystallites, determined in part 1. The infra-red dipole orientation with respect to the chain axis has been derived for several modes due to molecules in either the crystalline or the amorphous conformations. Combining the results with those of part 1 allows the conclusion that the development of molecular orientation in the present samples fits well into the general picture built up by other workers using a variety of somewhat different techniques for producing orientation.

(Keywords: poly(aryl ether ether ketone); PEEK; orientation; infra-red; conformations; crystallinity)

INTRODUCTION

Infra-red (i.r.) spectroscopy has been used in a number of investigations of the molecular vibrations, orientation, crystallization and melting behaviour of poly(aryl ether ether ketone) (PEEK).

Chalmers *et al.*¹ used i.r. reflection spectroscopy to investigate the percentage crystallinity of PEEK samples in the form of isotropic plaques by studying intensity changes of absorption peaks in the spectra. In particular, the crystallinity values for these samples, obtained by WAXS², were found to correlate well with the ratios of the absorbances at 1305 cm^{-1} (this peak was found to be closer to 1306 cm^{-1} in the present work) and 1280 cm^{-1} and at 970 and 952 cm^{-1} .

Nguyen and Ishida³ produced thin films by melt-casting PEEK at 400°C onto potassium bromide plates, and then quenching in liquid nitrogen. Some films were then annealed at various temperatures for various times in order to produce samples of different crystallinities. Spectra characteristic of the amorphous and crystalline phases were obtained by digital subtraction of a fraction

of a spectrum of an annealed sample from a spectrum of a quenched sample and vice versa. The fractions were determined by trial and error such that no negative absorbance peaks were seen in the difference spectra. Many differences were seen between the spectra characteristic of amorphous and crystalline material, such as differences in peak positions, relative intensities and sharpness, with the crystalline spectrum having the sharper peaks. Comparisons between the characteristic crystalline and amorphous spectra and spectra of model compounds for PEEK led Nguyen and Ishida^{3–5} to make tentative assignments of the absorption frequencies of PEEK.

No previous investigation of oriented samples of PEEK by i.r. spectroscopy has been reported, except by Nguyen and Ishida⁶ who studied PEEK crystallized on various substrates and found evidence for some orientation. The aim of the present investigation was to use i.r. spectroscopy to provide as much information as possible about the degree of molecular orientation and other structural features of uniaxially oriented PEEK, as well as providing further information that could aid spectral assignments. The results are discussed in conjunction with those for refractive index and X-ray studies of the same samples reported elsewhere⁷.

* To whom correspondence should be addressed

Table 1 Draw ratios, densities, mass fraction crystallinities and overall orientation of samples

Sample	Draw ratio, λ	Density, ρ_s (g cm^{-3})	Crystallinity, χ_m (%)	Overall orientation, $\langle P_2(\cos \theta) \rangle$
A	1.00	1.266	1.9	-0.02
B	1.40	1.267	2.8	0.17
C	1.79	1.268	3.8	0.25
D	2.10	1.272	7.5	0.36
E	2.45	1.280	14.9	- ^a
F	2.79	1.280	14.9	0.60
G	2.92	1.285	19.4	0.59
H (annealed)	2.92	1.314	45.3	0.78

^a Refractive indices for sample E were not determined accurately

EXPERIMENTAL

Samples

The preparation of the samples of PEEK used in this work has been described in detail in part 1⁷. Melt-cast film of thickness $\sim 7 \mu\text{m}$ was chosen to make the samples for drawing, which were cut with a dumb-bell cutter and drawn on an Instron tensile testing machine at 150°C at an initial strain rate of $40\% \text{ min}^{-1}$ to draw ratios in the range 1.00 to 2.92. In order to produce a sample of increased crystallinity a small section ($\sim 3 \text{ cm}$ long), was cut from a sample with draw ratio 2.92. It was held taut by clamps at either end and the sample and clamps were then placed in an air-circulating oven for $\sim 2 \text{ h}$ at 300°C . Table 1 shows the draw ratios of the samples produced.

The densities of the samples were measured using an aqueous potassium iodide density column. The values obtained are shown in Table 1 and are accurate to $\pm 0.003 \text{ g cm}^{-3}$. In calculating the crystallinities shown in Table 1 from these data the densities of crystalline and amorphous PEEK were taken to be 1.380 and 1.264 g cm^{-3} , respectively⁷.

Infra-red spectroscopy

All i.r. spectra were recorded on a Perkin-Elmer 580B ratio recording spectrometer purged to remove water vapour and carbon dioxide. The output was stored on a computer (PE 3600 Data Station) attached to and controlling the spectrometer. These data were then transferred to an Amdahl mainframe computer for processing. Spectra were recorded over the range $640\text{--}2000 \text{ cm}^{-1}$ with data points at intervals of 0.5 cm^{-1} . The resolution was $2.8 \pm 0.4 \text{ cm}^{-1}$ and all peaks studied in detail had a separation equal to or greater than this resolution.

In order to measure molecular orientation of polymer films by i.r. spectroscopy, polarized spectra must be obtained. To do this, two KRS-5 wire-grid polarizers were mounted in the spectrometer, one in the sample beam and one in the reference beam. They were both set at $45 \pm 0.5^\circ$ to the vertical to minimize effects due to the inherent polarization properties of the spectrometer.

The films of different draw ratios were mounted, in turn, on a square metal backing plate with a circular hole in the middle. The sample was mounted with its plane perpendicular to the incident i.r. beam in such a way that the draw direction could be set parallel or perpendicular to the polarization direction of the polarizer. The beam traversed the same part of the sample in either orientation

and the polarizers remained fixed. An attenuator was placed in the reference beam to compensate for the radiation blocked by the backing plate.

ANALYSIS OF SPECTRA

Preliminary considerations

Most spectra did not show interference fringes or showed them with very low amplitude, which may have been due to the roughness of the surfaces of the samples or to an unevenness in thickness. In order to ascertain the maximum difference that fringe correction would make to the orientation averages to be calculated, one spectrum of an isotropic film, which showed the most noticeable fringes, was treated by using the Kramers-Kronig integral method⁸ to remove the fringes. A computer program written by Dr I. Karacan was used for this purpose. Comparison of the 'corrected' spectrum with the 'uncorrected' spectrum revealed only small differences, with only a few peaks slightly reduced in intensity in the lower wavenumber region; it was therefore decided to neglect any further correction for fringes.

An increasing difference between parallel and perpendicular spectra with draw ratio was observed, showing that the samples became increasingly oriented with increasing draw ratio. Figure 1 shows the parallel and perpendicular spectra for samples D and F. The quantifying of these changes is considered below.

Computer curve fitting of spectra

Computer programs used. To enable calculations of the orientation average $\langle P_2(\cos \theta_\mu) \rangle = \frac{1}{2}(3\langle \cos^2 \theta_\mu \rangle - 1)$ to be made, where θ_μ is the angle between the transition moment for a particular vibrational mode and the draw direction, accurate values of the heights and widths of the peaks in the spectra were determined using a

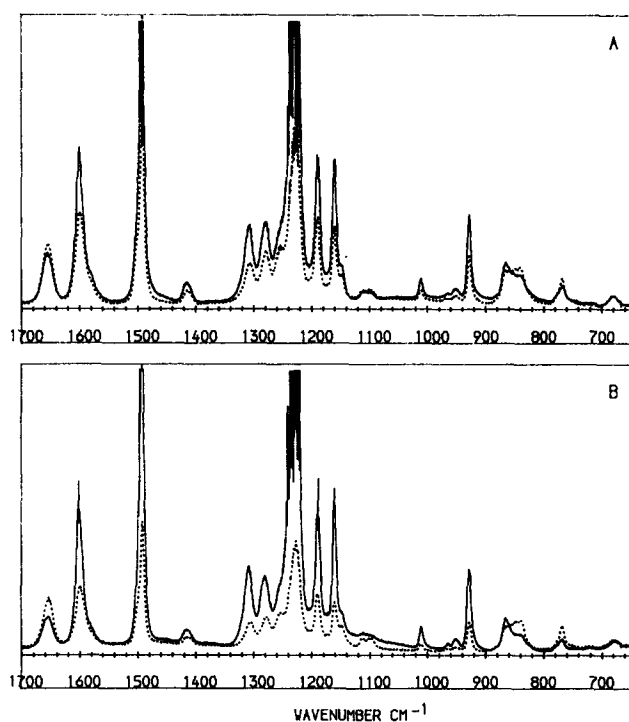


Figure 1 Parallel (—) and perpendicular (....) i.r. spectra of (A) sample D ($\lambda = 2.10$) and (B) sample F ($\lambda = 2.79$)

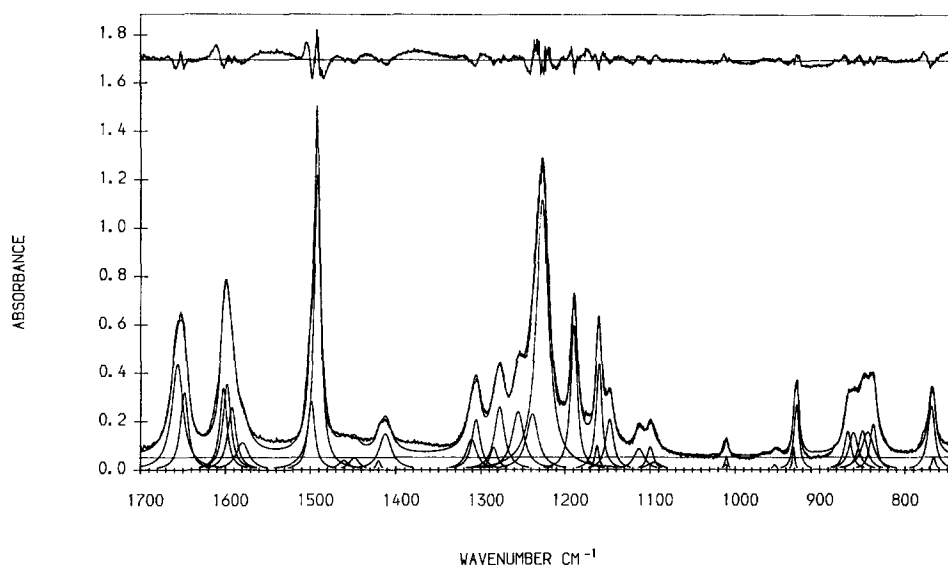


Figure 2 Perpendicular spectrum of sample F, fitted with crystalline and amorphous components. Top trace shows difference between fit and experimental data

computer program called FITTER (written by Dr P. Spiby). This program allowed a damped least-squares fit of overlapping Lorentzians with variable position, height and width (full width at half peak height), and allowed for a variable linear background.

Three versions of this program were used: HEIGHT, which allowed only the heights of the Lorentzians and the background to vary; RESTRICT, which allowed restricted variation of height, width, position and background; and CUVFIT which allowed unrestricted variation of all parameters.

To fit a spectrum, an initial estimate was made of the background, and of the height, width and position of each peak. Experience revealed that the best fitting procedure was to start with HEIGHT to obtain a better estimate of the heights and background, then to use RESTRICT to refine all the parameters further and finally to use CUVFIT to produce the best possible fit to the experimental data.

Separation of 'crystalline' and 'amorphous' peaks. When the fitting procedure was applied to the spectra of a highly drawn sample, F, fitting the obvious peaks visible in each spectrum, a number of peaks could be fitted with approximately the same wavenumber position in the parallel and perpendicular spectra; on the other hand a shift of more than 1 cm^{-1} was found between many pairs of corresponding peaks in the two spectra. This suggested that most obvious peaks really consist of two components, one due to a 'crystalline' vibration and one due to an 'amorphous' vibration, as reported by Nguyen and Ishida³. The quotation marks imply vibrations of chains with the crystalline or amorphous conformation rather than vibrations due to the crystalline or the amorphous phases. The apparent shifts in position from parallel to perpendicular spectrum could then be explained by the 'amorphous' and 'crystalline' material orienting at different rates with draw ratio.

The parallel and perpendicular spectra of sample F were then each fitted independently with two Lorentzians to most of the obvious peaks. The initial positions of these Lorentzian peaks were chosen as those suggested by Nguyen and Ishida³, although the computer fitting

allowed the peak positions to vary. *Figure 2* shows the fitted perpendicular spectrum for sample F. This method resulted in a better fit to the experimental data, with most peaks having less than 1 cm^{-1} shift between the parallel and perpendicular spectra. The peaks that did show a greater shift were either very small, or too large to be recorded accurately by the spectrometer, or just badly fitted. Although this gave some support for the ideas of Nguyen and Ishida, fitting with more peaks will always give a better fit. To examine further the idea that each obvious peak consisted of two overlapping components, several more tests were made.

1. Samples A, G and H had very different crystallinities, namely $\sim 2, 19$ and 45% , respectively. The parallel and perpendicular spectra of each sample were combined to produce the spectrum of an effectively isotropic sample, i.e. as if unoriented but with the same crystallinity and conformational distribution as the real sample. The samples were shown in part 1 to be uniaxially oriented and the 'isotropic' spectrum is then given by:

$$\text{Isotropic spectrum} = \frac{1}{3} \left[\left(\begin{array}{c} \text{parallel} \\ \text{spectrum} \end{array} \right) + 2 \left(\begin{array}{c} \text{perpendicular} \\ \text{spectrum} \end{array} \right) \right] \quad (1)$$

The resulting isotropic spectra were standardized by dividing by the thickness of the sample. *Figure 3* shows that there is a shift of peak position from sample A to H consistent with Nguyen and Ishida's idea of 'crystalline' and 'amorphous' peaks, i.e. as the crystallinity of the sample increases the isotropic peaks shift towards the 'crystalline' wavenumber and away from the 'amorphous' wavenumber. Fitting these isotropic spectra with two Lorentzians per obvious peak showed that on the whole the 'crystalline' components rise and the 'amorphous' components fall with increasing crystallinity.

2. Nguyen and Ishida's spectral subtraction method³ was also used to separate the peaks of the spectrum into those characteristic of the 'amorphous' vibrations and those characteristic of the 'crystalline' vibrations, using the isotropic spectra obtained for samples A and G as one pair and those obtained for samples A and H as another pair of spectra corresponding to very different

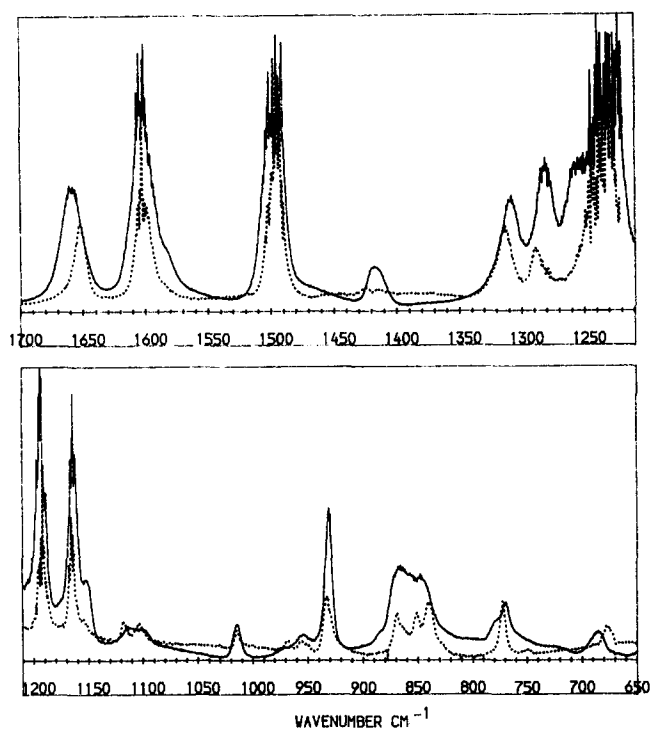


Figure 3 Isotropic spectra for samples A (—) and H (.....) showing shifts in peak positions with increasing crystallinity

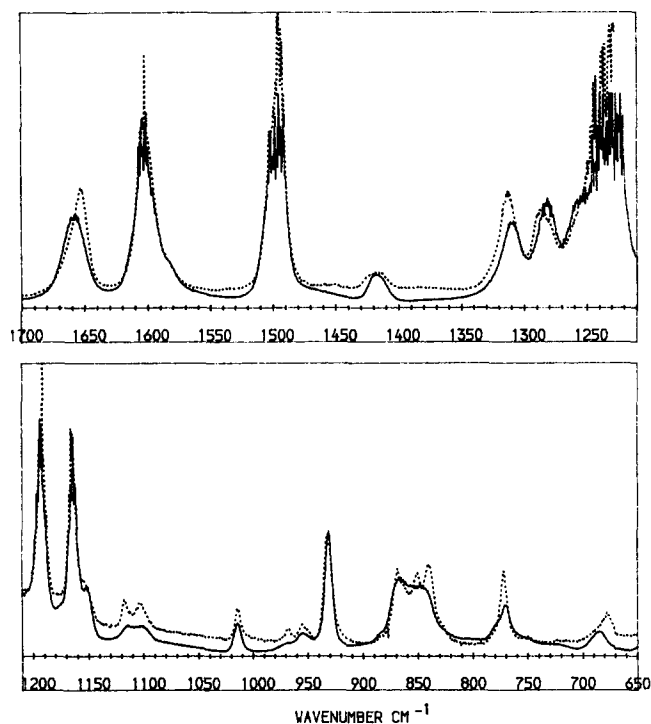


Figure 4 Spectra characteristic of crystalline (.....) and amorphous (—) conformers

crystallinities. Good agreement was found between the two 'amorphous' spectra and between the two 'crystalline' spectra thus obtained. There is a definite difference between the positions in the 'amorphous' spectrum and those in the 'crystalline' spectrum and many peaks in the 'crystalline' spectrum are narrower than the corresponding peaks in the 'amorphous' spectrum, as seen in Figure 4. The characteristic spectra obtained here agree closely with those obtained by Nguyen and Ishida³.

3. Finally, the 'amorphous' and 'crystalline' spectra were fitted with a single Lorentzian per obvious peak, since each spectrum should now contain only one of the two components present in the original spectra, unlike the isotropic spectra in (1). The results are shown in Table 2. Uncertainties in peak positions were $<0.4 \text{ cm}^{-1}$ (estimated by doing one further CUVFIT iteration once a good fit had been found, and comparing the positions between one good fit and another). The table omits peaks that were very badly fitted. Peak positions along a horizontal row in Table 2 apply to the same obvious peak. There is good agreement between the two 'amorphous' positions in most cases. The 'crystalline' positions are not always so close to each other, but the shift between 'amorphous' and 'crystalline' positions is greater than the different between the two 'amorphous' positions in most cases.

From all this evidence it was concluded that most of the obvious peaks in the spectrum of PEEK consist of two components, one due to a vibration of molecules in the crystalline conformation and one due to a vibration of molecules in the amorphous conformation, as suggested by Nguyen and Ishida.

Final fitting of spectra. The parallel and perpendicular spectra of the remaining samples A–H were fitted with 'crystalline' and 'amorphous' peaks by the method described above under 'Computer programs used'. No trend of shift in position or width with draw ratio was noticed except a slight narrowing of some of the peaks for sample H, the most crystalline. The position and width of each peak was therefore averaged over all the samples and all spectra were refitted with these averaged peak positions and widths using HEIGHT only. Table 3 shows these final average peak positions and widths.

Calculation of orientation averages $\langle P_2(\cos \theta_\mu) \rangle$

Orthogonal axes $OX_1X_2X_3$ are chosen in the drawn samples with OX_3 parallel to the draw direction and OX_1 lying in the plane of the film. For samples with uniaxial symmetry around OX_3 the value of $\langle P_2(\cos \theta_\mu) \rangle$ is given

Table 2 Positions (cm^{-1}) of peaks in characteristic 'amorphous' and 'crystalline' spectra

'Amorphous'		'Crystalline'	
Samples A and G	Samples A and H	Samples A and G	Samples A and H
1655.9	1656.1	1653.2 ^a	1649.4
1599.7	1600.2	1601.1	1600.7
1583.7 ^a	1588.3 ^a	1593.8 ^a	1594.4 ^a
		1496.3	1498.7
1494.1	1494.0	1491.6	1491.7
1414.3	1414.3		
1307.4	1307.1	1309.2	1311.2
1279.4	1279.3	1280.2 ^a	1285.2 ^a
1225.6	1225.9	1226.2	1226.3
1190.0	1189.9	1189.9	1188.3
1160.7	1160.6	1161.0	1161.7
1110.9	1110.7	1113.8 ^a	1114.8
953.0	952.5	953.1 ^a	952.8 ^a
928.2	928.2	928.3 ^a	929.3
864.3 ^a	863.8 ^a	865.3 ^a	865.2 ^a
843.9 ^a	843.5 ^a	850.4 ^a	848.5 ^a
767.6 ^a	765.9 ^a	769.1	769.3

^a Poor fit

Table 3 Average fitted peak positions and halfwidths for PEEK

Peak ^a	Position (cm ⁻¹)	Halfwidth (cm ⁻¹)	Peak ^a	Position (cm ⁻¹)	Halfwidth (cm ⁻¹)
A	1657.0	16	C	1162.3	6
C	1648.8	9	A	1160.2	8
C	1602.3	10	A	1147.6	11
A	1598.3	11	C	1113.1	15
C	1592.2	12	C	1099.9	9
A	1579.5	18	A	1095.3	20
C	1498.8	10	C	1011.5	6
CA	1492.2	9	A	1010.5	4
C	1460.5	15	C	966.7	12
C	1448.3	14	C	953.4	6
C	1420.2	6	A	952.8	9
A	1414.9	11	C	947.8	7
C	1412.2	17	C	930.7	3
C	1311.3	15	A	927.7	7
A	1305.7	12	C	867.1	10
C	1284.7	11	A	860.0	13
A	1277.8	14	C	849.2	12
A	1255.7	17	A	843.1	17
C	1238.8	17	C	837.1	15
CA	1227.1	17	C	769.3	10
CA	1189.5	9	A	766.4	5

^a A and C refer to 'amorphous' and 'crystalline' peaks, respectively. The peaks assigned to different types of vibrations are grouped

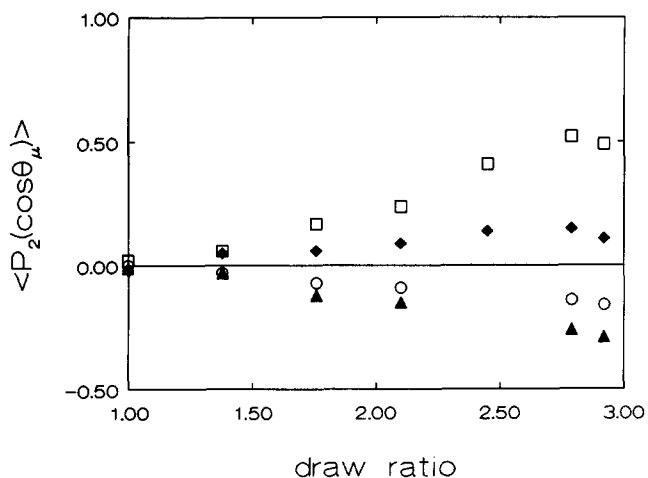


Figure 5 $\langle P_2(\cos \theta_\mu) \rangle$ for the crystalline and amorphous conformers plotted against draw ratio for the pairs of peaks at 1649/1657 cm⁻¹ ((▲) crystalline, (○) amorphous) and 1285/1278 cm⁻¹ ((□) crystalline, (◆) amorphous)

by⁹

$$\langle P_2(\cos \theta_\mu) \rangle = \frac{\phi_3 - \phi_1}{\phi_3 + 2\phi_1} \quad (2)$$

where

$$\phi_i = \frac{6n_i k_i}{(n_i + 2)^2 + (2n_i^2 - 4)k_i^2 + k_i^4} \quad (3)$$

for $i = 1$ or 3 . In this equation n_1 and n_3 are the principal refractive indices at the wavenumber ν of the absorption peak and

$$k_i = A_i / (4\pi\nu t \log_{10} e) \quad (4)$$

where A_i is the height (absorbance) of the peak and t is the thickness of the sample.

Calculations of $\langle P_2(\cos \theta_\mu) \rangle$ were made separately for the 'crystalline' and 'amorphous' components of each peak. The value of n_1 was approximated by the average of the experimental values of n_1 and n_2 found in the visible region in part 1. Only peaks that were fairly well fitted were used in this analysis. Figure 5 shows the trend of $\langle P_2(\cos \theta_\mu) \rangle$ with draw ratio for the 'crystalline' and 'amorphous' components $\langle P_2(\cos \theta_\mu) \rangle_c$ and $\langle P_2(\cos \theta_\mu) \rangle_a$, respectively for the peaks at 1649/1657 and 1285/1278 cm⁻¹ and the values for the first pair are listed in Table 4. For most pairs of peaks the 'crystalline' orientation was found to be higher than the 'amorphous' orientation and the exceptions were generally the less well fitted peaks.

The orientation averages calculated so far are for the transition moments of the vibrations and not for the molecular chains. In order to obtain the orientation average of the chains the following equation was used, where θ_m is the angle between a particular transition moment and the chain axis:

$$\langle P_2(\cos \theta) \rangle = \langle P_2(\cos \theta_\mu) \rangle / P_2(\cos \theta_m) \quad (5)$$

Use of this equation implies that there is no preferred orientation of the chains around the chain axis. It was shown in part 1 that the crystallites have no preferred orientation around the c axis and it is assumed that the amorphous chains also do not have any preferred orientation around the chain axis.

The only vibration for which the angle between the transition moment and the chain axis is known with any certainty is the stretch of the carbonyl group at 1649/1657 cm⁻¹. Molecular symmetry predicts the angle to be 90° for the vibration of the molecules in the crystalline conformation. The orientation average of the molecular chains in the crystalline conformation can thus be calculated by dividing the i.r. orientation average, $\langle P_2(\cos \theta_\mu) \rangle_c$, for this peak by -0.5 . The resulting values of chain orientation for the crystalline conformers, $\langle P_2(\cos \theta) \rangle_c$, are listed in Table 4 and plotted in Figure 6 along with the crystalline and amorphous phase orientation averages from part 1. The average orientation determined in part 1 from refractive index data is represented by the solid line.

Crystallinity from i.r. spectroscopy

From absorbance ratios. In an attempt to obtain crystallinity values from multiple internal reflection i.r. spectra of PEEK, Chalmers *et al.*¹ plotted the intensity ratios of the peaks at 1306 and 1280 cm⁻¹ and at 970 and 952 cm⁻¹ against percentage crystallinity as determined from WAXS. A straight line correlation was obtained for

Table 4 Orientation averages calculated from data for the peaks at 1649/1657 cm⁻¹

Sample	$\langle P_2(\cos \theta_\mu) \rangle_a$	$\langle P_2(\cos \theta_\mu) \rangle_c$	$\langle P_2(\cos \theta) \rangle_c$
A	-0.00	-0.00	0.00
B	-0.03	-0.03	0.06
C	-0.07	-0.12	0.24
D	-0.09	-0.15	0.30
E	-0.10	-0.22	0.44
F	-0.14	-0.26	0.52
G	-0.16	-0.29	0.58
H	-0.16	-0.46	0.92

Subscripts a and c refer to chains in amorphous and crystalline conformations, respectively

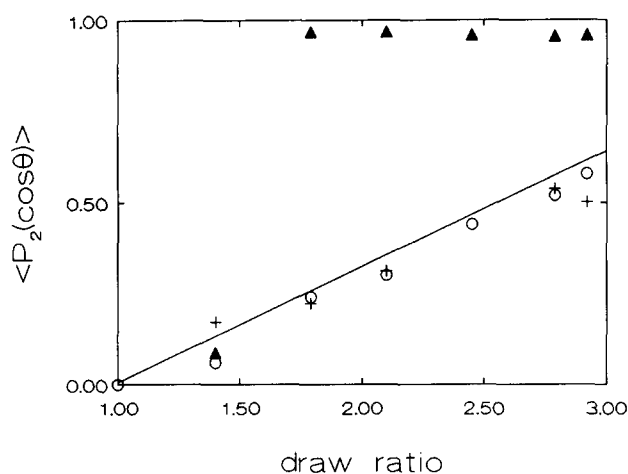


Figure 6 $\langle P_2(\cos\theta) \rangle$ plotted against draw ratio: (▲) crystalline phase⁷; (+) amorphous phase⁷; (○) crystalline conformers ($\langle P_2(\cos\theta) \rangle_c$). The straight line represents the variation of average orientation from refractive index data⁷

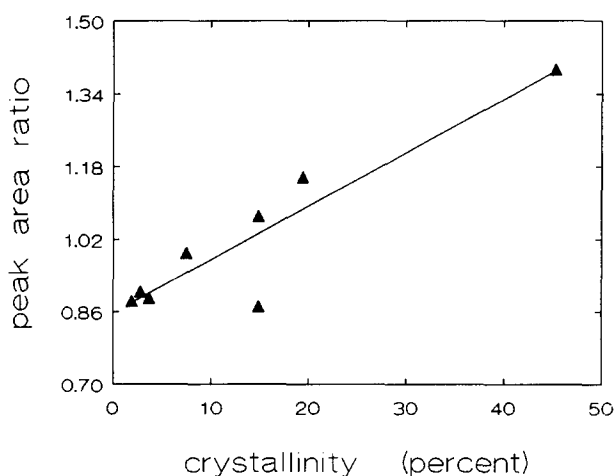


Figure 7 1306/1280 cm^{-1} peak area ratio plotted against mass fraction crystallinity from density

each pair of peaks; slightly different slopes were obtained for the two pairs, 0.0083 and 0.0090, respectively.

A graph was plotted of the ratio of the areas of the 1306 and 1280 cm^{-1} peaks obtained in the present work against the mass fraction crystallinity. The 970/952 cm^{-1} peaks were too small for any quantitative analysis. The areas of the peaks at 1306 and 1280 cm^{-1} were calculated by adding together the areas of the separate 'crystalline' and 'amorphous' components of each peak. The area of each component was obtained by combining the parallel and perpendicular heights to give the isotropic absorbance and then multiplying by the width $\Delta_{1/2}$. Thus the ratio of the areas is given by;

$$\frac{\text{area of 1306}}{\text{area of 1280}} = \frac{\{[(\phi_3 + 2\phi_1)\Delta_{1/2}]_c + [(\phi_3 + 2\phi_1)\Delta_{1/2}]_a\}_{1306}}{\{[(\phi_3 + 2\phi_1)\Delta_{1/2}]_c + [(\phi_3 + 2\phi_1)\Delta_{1/2}]_a\}_{1280}} \quad (6)$$

Figure 7 shows this ratio of areas plotted against the mass fraction crystallinity (expressed as a percentage) as obtained from density. A least-squares fit of these data yields a slope of 0.012 ± 0.002 . A reasonable straight line correlation is achieved, although not as good as that obtained by Chalmers *et al.* The slope obtained here is slightly higher than that obtained by them but this is

most probably due to the different methods employed in determining both the absorbance ratios and the crystallinities.

From fitted 'crystalline' and 'amorphous' components.

The ratio of the areas of the 'crystalline' and 'amorphous' components of a peak should be related to the crystallinity. Table 5 shows the quantity $\chi^* = C/(C + A)$, expressed as a percentage, for 10 fairly well fitted peaks for samples A to H, where C and A refer to the total areas of the 'crystalline' and 'amorphous' fitted components respectively, and are given by:

$$C = \frac{1}{3}[(\phi_3 + 2\phi_1)\Delta_{1/2}]_c, \quad A = \frac{1}{3}[(\phi_3 + 2\phi_1)\Delta_{1/2}]_a \quad (7)$$

Sample H has the highest χ^* value, as expected, for all pairs of peaks except 1620/1598 cm^{-1} and 1592/1580 cm^{-1} . These two pairs overlap and this may have affected the fitting. The orientation data for the latter pair is also anomalous, as is the orientation data for the 769/766 cm^{-1} pair. From now on the data from these three pairs of peaks will be neglected, as will those for the pairs at 867/860 and 849/845 cm^{-1} , which gave rather poor fits.

The pairs of peaks at 1649/1657, 1311/1306 and 1285/1278 cm^{-1} , which are well fitted, show a definite increase in χ^* with draw ratio. These values of χ^* , the percentage of crystalline conformers, are not only greater than the crystallinity, χ_m , of the corresponding sample, as expected, but the values of χ^* for each sample differ widely over the peaks considered. This suggests that either different lengths of chain are required to be straight in order to contribute to the 'crystalline' component and/or that the 'crystalline' and 'amorphous' components have different extinction coefficients. The latter possibility is supported by the fact that $(C + A)$ varies with draw ratio. The fraction of crystalline conformers should thus be given by $\chi_{ir} = PC/(PC + A)$, where P is equal to the ratio of the extinction coefficients of the 'amorphous' and 'crystalline' components of a peak.

Since $(PC + A)/\rho_s$ should be constant, where ρ_s is the density of the sample, it should be possible to obtain a value of P from a least-squares fit to a plot of A/ρ_s against C/ρ_s . Figure 8 shows the graph plotted for the peaks at 1649/1657 cm^{-1} , Table 6 shows the values of P obtained for the five pairs of peaks considered and Table 7 shows the corrected values of crystalline conformer content χ_{ir} . The use of the P factors reduces the range of values of crystalline conformer content for each sample obtained from the different pairs of peaks. The remaining differences between one pair and another may be due to

Table 5 Values of $\chi^* = C/(C + A)$ for selected peaks for samples A to H, expressed as percentages

Peaks	$\chi^* = C/(C + A)$ for sample							
	A	B	C	D	E	F	G	H
1649 1657	14	18	18	21	25	25	26	48
1602 1598	62	55	52	52	48	48	51	41
1592 1580	68	65	68	69	68	63	68	71
1311 1306	46	47	48	52	58	57	61	80
1285 1278	19	20	20	21	26	26	28	48
1162 1160	21	21	23	26	27	23	23	36
931 928	11	7	8	8	12	15	14	21
867 860	51	50	49	51	51	52	52	58
849 845	44	51	43	49	40	41	42	71
769 766	89	83	83	85	88	89	90	96

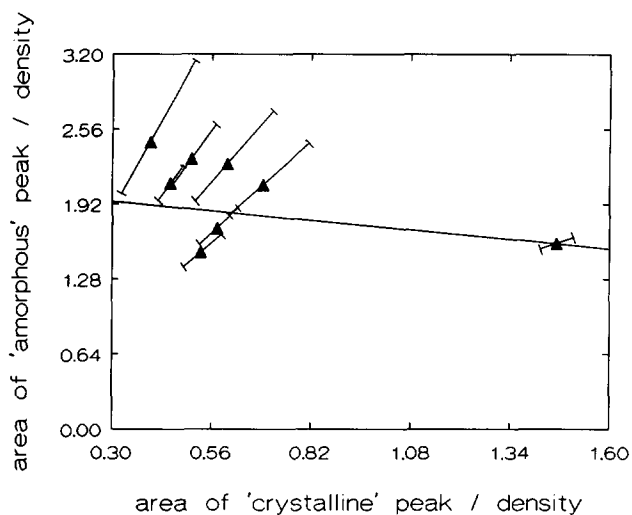


Figure 8 Graph used to obtain the *P* value for the pairs of peaks at 1649 and 1657 cm^{-1}

Table 6 Values of *P* for the well fitted pairs of peaks, where *P* is the ratio of the extinction coefficients for corresponding 'amorphous' and 'crystalline' peaks

Peaks		<i>P</i>
1649	1657	0.31 ± 0.10
1311	1306	0.22 ± 0.03
1285	1278	0.63 ± 0.11
1162	1160	0.76 ± 0.25
931	928	1.29 ± 0.38

Table 7 Crystalline conformer content χ_{ir} , expressed as a percentage, for samples A to H

Peaks	$\chi_{ir} = PC/(PC + A)$ for samples							
	A	B	C	D	E	F	G	H
1649 1657	4.8	6.4	6.3	7.6	9.4	9.4	9.8	22.3
1311 1306	15.8	16.3	16.9	19.3	23.3	22.6	25.6	46.8
1285 1278	12.8	13.6	13.6	14.3	18.1	18.1	19.7	36.8
1162 1160	16.8	16.8	18.5	21.1	22.0	21.1	18.5	29.9
931 928	13.8	8.8	10.1	10.1	14.9	18.5	17.4	25.5
Average χ_{ir}	12.8	12.4	13.1	14.5	17.5	17.9	18.2	32.3
χ_m	1.9	2.8	3.8	7.5	14.9	14.9	19.4	45.3

Table 8 Crystallinity values from i.r. peaks

Peaks	$\chi_{IR} = (PC - RA)/(PC + A)$ for samples								
	A	B	C	D	E	F	G	H	
1649 1657	0	1.7	1.6	3.0	4.9	4.8	5.3	18.4	
1311 1306	0	0	1.1	3.9	8.7	7.3	11.5	36.7	
1285 1278	0	0.6	0.6	1.4	5.8	5.8	7.6	27.3	
1162 1160	0.2	0.2	2.2	5.3	6.3	5.3	2.2	15.9	
931 928	5.1	0.3	1.1	1.1	6.4	10.4	9.1	18.1	
Average χ_{IR}	1.1	0.6	1.3	2.9	6.4	6.7	7.1	23.3	
χ_m	1.9	2.8	3.8	7.5	14.9	14.9	19.4	45.3	
<i>R</i>	0.13	0.11	0.11	0.08	0.03	0.04	-0.01	-0.19	

the fact that different lengths of straight chain are needed in each case in order to contribute to the 'crystalline' component. The average values for each sample are shown at the bottom of the table, together with the values of χ_m from Table 1 for comparison.

The major problem associated with the calculation of *P* is the large uncertainty in the thickness of the samples, which were on average only 4 μm thick. These uncertainties in thickness are represented in Figure 8 by the error bars on each point and lead to uncertainties in the values of χ_{ir} which vary from ~6 to 30%, depending on the sample and pair of peaks involved.

It is seen that χ_{ir} is $\geq \chi_m$ for all samples, within experimental uncertainty, confirming that not all crystalline conformers are contained in crystallites. The value of χ_m is approximately constant up to a draw ratio of 2 and at draw ratios above this it increases rapidly. A hint of a similar trend is seen with χ_{ir} .

The simplest assumption that can be made in attempting to obtain true crystallinity measurements from the i.r. data is that the ratio of crystalline to amorphous conformers in the amorphous phase remains constant for each peak. This assumption is consistent with the assumption of constant density for the amorphous phase in the two phase model. The crystallinity from i.r. data is then given by

$$\chi_{IR} = (PC - RA)/(PC + A) \quad (8)$$

where *R* is the ratio of crystalline to amorphous conformers in the amorphous phase and is taken as the ratio of *PC/A* obtained from sample A or B, whichever gave the lower value.

Table 8 shows the values of χ_{IR} calculated for the peaks in Table 6 together with the average values over all five pairs of peaks and the values of χ_m . The values of χ_{IR} tend to be too low at high draw ratios, which suggests that the value of *R* is not constant. It is easy to show that the value of *R* required to give exact agreement between χ_{IR} and χ_m is given by

$$R = (\chi_{ir} - \chi_m)/(1 - \chi_{ir}) \quad (9)$$

Using the average values of χ_{ir} for each sample leads to the values of *R* shown at the bottom of Table 8. They are plotted against χ_m in Figure 9 and an approximate straight line is found, suggesting strongly that the ratio of crystal conformers to amorphous conformers within the amorphous material falls quite rapidly as orientation and crystallinity develop on drawing. The *R* value obtained for the annealed sample H is negative, and the

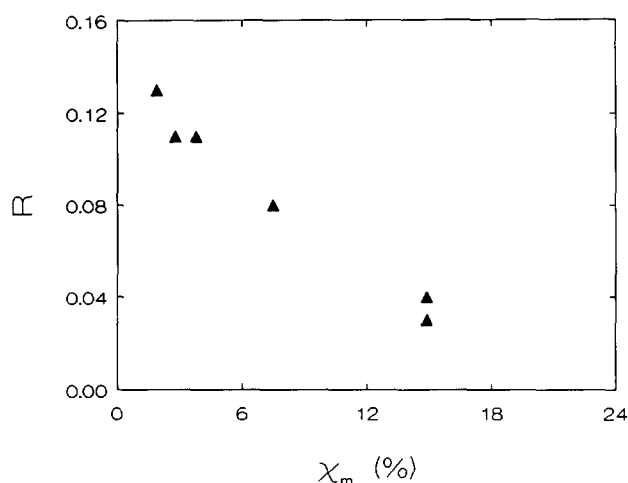


Figure 9 Variation of straight chain content in the amorphous phase (R), given by equation (9), plotted against mass fraction crystallinity

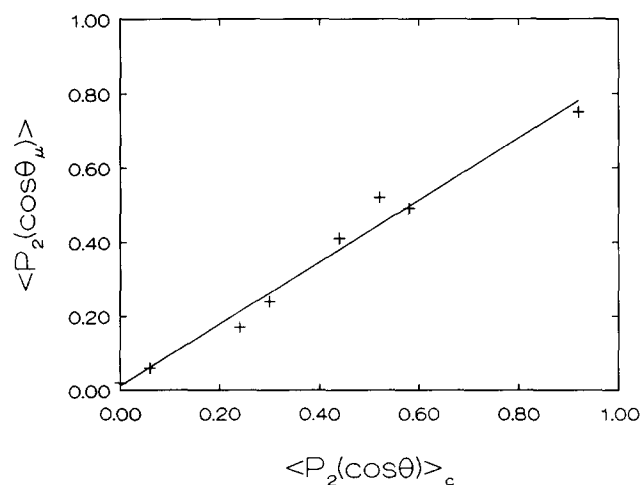


Figure 10 The orientation average $\langle P_2(\cos \theta_\mu) \rangle_c$ of the transition moment for the crystalline conformer absorption at 1285 cm^{-1} plotted against the orientation average $\langle P_2(\cos \theta) \rangle_c$ for the axes of the crystalline conformers

reason for this is unclear. If, however, $R=0$, $\chi_{\text{IR}} = \chi_{\text{ir}}$, and Table 7 shows that allowing for the uncertainty in χ_{ir} there is reasonable agreement with χ_{m} .

Infra-red transition dipole angles

Equation (5) shows that if $\langle P_2(\cos \theta) \rangle$ is known it is possible to calculate the angle between the transition dipole moment and the chain axis for any vibration for which $\langle P_2(\cos \theta_\mu) \rangle$ is known. A measure of $\langle P_2(\cos \theta) \rangle$ for the crystalline conformers, $\langle P_2(\cos \theta) \rangle_c$, has already been obtained from the i.r. data for the 'crystalline' component of the carbonyl stretching peak at 1649 cm^{-1} , for which the vibrational dipole is normal to the chain axis. The value of $P_2(\cos \theta_m)$ for each of the remaining 'crystalline' components may be obtained from the slope of a graph of $\langle P_2(\cos \theta_\mu) \rangle_c$, the orientation average of the transition moment of the 'crystalline' component, versus $\langle P_2(\cos \theta) \rangle_c$. The angle θ_m can then be calculated. Figure 10 shows the graph for the peak at 1285 cm^{-1} .

Reasonable straight line graphs were obtained for all 10 'crystalline' peaks listed in Table 5 (with the possible exception of that at 1592 cm^{-1} for which the data points were slightly erratic), suggesting that the angle between transition moment and chain axis for the crystalline

conformers remains constant with draw ratio, as expected. The values of θ_m thus obtained are shown in Table 9.

In order to calculate θ_m for the amorphous conformers it is necessary to know the orientation average of the chains in the amorphous conformation. This was obtained by use of the equation:

$$\langle P_2(\cos \theta) \rangle = \chi_{\text{ir}} \langle P_2(\cos \theta) \rangle_c + (1 - \chi_{\text{ir}}) \langle P_2(\cos \theta) \rangle_a \quad (10)$$

where $\langle P_2(\cos \theta) \rangle$ is the average orientation of the whole sample, obtained in part 1 from refractive indices, and $\langle P_2(\cos \theta) \rangle_a$ is the orientation average of chains in the amorphous conformation. Equation (5) was then used with $\langle P_2(\cos \theta) \rangle_a$ and $\langle P_2(\cos \theta_\mu) \rangle_a$ to calculate the values of θ_m for the chains in the amorphous conformation and the results obtained are also shown in Table 9.

Straight line graphs were obtained for the peaks at 1657 , 1306 , 1278 and 1160 cm^{-1} and the peak at 928 cm^{-1} gave a reasonable straight line. The values of θ_m for these five peaks are different from the corresponding angles for the crystalline conformers. In particular, the value for the carbonyl vibration at 1657 cm^{-1} is much less than 90° . The remaining peaks gave erratic graphs and no significance is attached to the resulting values of θ_m .

DISCUSSION AND CONCLUSIONS

The nature of the spectrum

The present work supports the conclusion of Nguyen and Ishida that the spectrum of PEEK may be regarded as the sum of two overlapping spectra, due to molecules in amorphous and crystalline conformations. This conclusion has been tested not only by their method of spectral subtraction for samples with different degrees of crystallinity but also by curve resolution. It accounts not only for the apparent shift in the obvious peaks with change of crystallinity but also for the apparent shift with change of polarization direction for oriented samples.

Conformational content and degree of crystallinity

The areas under the peaks characteristic of amorphous and crystalline conformations have been used to derive the fraction of material in the two conformational states and it is clear that the content of crystalline conformers is greater than the degree of crystallinity except for the most highly oriented sample and the annealed sample.

Table 9 Values of θ_m for crystalline and amorphous conformers

Peaks ^a (cm^{-1})		Crystalline θ_m (degrees)	Amorphous θ_m (degrees)
C	A		
1649 ^b	1657 ^b	(90)	65 ± 3
1602	1598	30 ± 2	
1592	1580	61 ± 2	
1311 ^b	1306 ^b	22 ± 4	45 ± 4
1285 ^b	1278 ^b	14 ± 7	45 ± 4
1162 ^b	1160 ^b	0 ± 10	40 ± 4
931 ^b	928 ^b	25 ± 7	32 ± 5
867	860	45 ± 2	
849	845	76 ± 4	
769	766	76 ± 3	

^a C, crystalline; A, amorphous

^b Well fitted peaks

It is not, however, possible to assume that there is a constant proportion of these conformers in amorphous material. It appears that this proportion falls roughly linearly with the degree of crystallinity deduced from density measurements.

Michele and Vittoria¹⁰ have undertaken a study of PEEK by means of wide-angle X-ray scattering, differential scanning calorimetry and the transport properties of dichloromethane vapour. They conclude that PEEK contains not only crystalline and amorphous phases, but also an intermediate phase which they call the 'rigid amorphous' phase. It seems likely that this rigid amorphous phase is related to the crystalline conformers present in the amorphous phase.

The linear relationship found by Chalmers *et al.* between the ratio of the absorbances at 1306 and 1280 cm^{-1} and the degree of crystallinity has been examined in more detail by using peak areas rather than peak heights. A similar linear relationship was found. The reason why these two peaks respond favourably to both methods is most probably due to their different P values (the ratio of the extinction coefficient of the 'amorphous' component to that of the 'crystalline' component). The peak at 1306 cm^{-1} has a P value of 0.22 whereas the peak at 1280 cm^{-1} has a P value of 0.63. This implies that the peak at 1306 cm^{-1} is much more sensitive to crystalline conformers than the one at 1280 cm^{-1} , and hence the ratio of the area of the peak at 1306 cm^{-1} to that at 1280 cm^{-1} will increase with increasing crystallinity.

Orientation

The average orientation of the chains in the crystalline conformation is very much lower than that of the chains in the crystallites for all except possibly the least oriented sample. Since there are more chains with this conformation in actual crystalline material than in amorphous material for more highly drawn samples, the orientation of those chains that are in the amorphous regions must be very low. The average orientation of all chains in the crystalline conformation is in fact close to the overall average orientation of all chains determined from refractive indices and to the overall amorphous orientation determined by combining refractive index, X-ray and crystallinity data, the latter being deduced from density measurements.

Infra-red dipole orientations

The line group of the single chain in the crystalline conformation has a factor group isomorphous with the group C_{2h} . Infra-red active modes thus fall into two symmetry species, A_u with the transition moment perpendicular to the chain axis and parallel to the direction of the C=O bond and B_u with the transition moment anywhere in the plane perpendicular to that direction. For a molecule as complicated as PEEK, with six closely coupled phenylene rings per repeat unit, spectral assignments and predictions of transition dipole directions on the basis of simple group vibrations are unlikely to be successful, with the exception of the assignment of the perpendicular mode that is essentially $\nu(\text{C}=\text{O})$ and occurs at 1649 cm^{-1} . This mode was found to have the highest negative dichroism of all the well fitted peaks, as expected for an A_u mode.

There appear to be no vibrational calculations for PEEK in the literature with which to compare the dipole

directions shown in Table 9. The only attempted assignments are those of Nguyen and Ishida on the basis of model compounds. The dipole directions in Table 9 should be useful in connection with future vibrational calculations where these attempt to calculate dipole directions as well as vibrational frequencies.

Summary of deformation of PEEK upon drawing

Combining the results of parts 1 and 2 gives the following picture of the deformation of amorphous PEEK film upon uniaxial drawing at a temperature of 150°C:

1. As the film begins to draw the amorphous chains are uncoiled and rotated towards the draw direction; this is suggested by the increase in amorphous orientation and by the increase in orientation of the amorphous and crystalline conformers as revealed by the i.r. analysis. The drawing temperature was deliberately above T_g to allow this movement of molecules. At first, no (or very few) crystals are formed, as shown by the slow initial rise in density, and the percentage content of crystalline conformers rises slowly. This complexity, where the drawing process involves both conformational changes and rotation of units, explains why neither the deformation of a rubber-like network nor the simpler rotation of rigid rods provides a satisfactory model for the development of orientation.
2. As a draw ratio of approximately 2 is reached, the crystallinity begins to increase much more rapidly because the degree of orientation of the crystalline conformers is such that regions exist in which the molecules are so well aligned that they can fall into crystal register. These crystals are approximately fully oriented even on creation, as shown by a crystalline orientation average of 0.97 for all draw ratios greater than 1.75.
3. Further drawing continues to increase the orientation of both crystalline and amorphous conformers and the percentage content of crystalline conformers, thus bringing more and more chains into a position where they can form crystals. At draw ratios above 3, the increase in crystallinity slows down a little.
4. The limit of extensibility of the samples is reached at a draw ratio of approximately 3.2, above which PEEK could not be drawn at the temperature and strain rate employed here.

Comparing this deformation of PEEK with that reported in the literature reveals good agreement with Ohkoshi *et al.*^{11,12}. They found that on drawing amorphous PEEK filaments, the birefringence varied linearly with draw ratio up to $\lambda \sim 3$ (a result also found in this work), although their values of birefringence are all slightly lower than those attained in this work. Ohkoshi *et al.* also found the onset of crystallinity to occur at a draw ratio of 2.

On the other hand, the deformation described above is in slight disagreement with that reported by Lee *et al.*¹³ for the extrusion of *initially crystalline* films and rods of PEEK at 154 and 310°C, respectively. They report an initial decrease in density (and hence crystallinity) on extrusion of the films and explain this as due to the destruction of lamellae. At higher draw ratios they find the crystallinity increases and consider this due to the production of chain-extended crystals (the nature of which they do not describe). The crystalline orientation averages reported by Lee rise with increasing draw ratio, but more slowly than for the samples studied in the present work. Lee quotes the crystalline orientation (as

measured by wide-angle X-ray diffraction) as levelling out at draw ratios ≥ 4 and then only with $\langle P_2(\cos \theta) \rangle \sim 0.7$.

It is perhaps also worth noting the comparison of the present results with those of three other groups of researchers who have drawn PEEK. Kunugi *et al.*¹⁴ have used the techniques of zone-drawing and zone-annealing on initially amorphous PEEK film, 110 μm thick. They have drawn at a temperature of 140°C and annealed at temperatures between 200 and 280°C. They have not quantitatively measured the molecular orientation attained, but X-ray photographs show a high degree of crystalline orientation. They also quote a maximum measured birefringence of 0.298 which is higher than that obtained in the present work (0.236). On the other hand, Kunugi *et al.* quote a maximum crystallinity of 35.1% whereas in the present work the maximum crystallinity achieved was 45.3%.

Rueda *et al.*¹⁵ have die drawn PEEK rods and qualitatively measured orientation by X-ray diffraction, showing that the crystalline orientation increases with draw ratio. Zhen *et al.*¹⁶ have drawn fibres of PEEK at 240°C. They obtain a maximum measured birefringence of 0.23 which is in very close agreement with the value found here (0.236).

ACKNOWLEDGEMENTS

The authors are grateful to ICI Advanced Materials Centre, Wilton for supplying materials, for making equipment and expertise available to them and for

providing some financial support for A.M.V. They wish to thank the SERC for a research grant for work on oriented polymers and for providing support for A.M.V.

REFERENCES

- 1 Chalmers, J. M., Gaskin, W. F. and Mackenzie, M. W. *Polym. Bull.* 1984, **11**, 433
- 2 Blundell, D. J. and Osborn, B. N. *Polymer* 1983, **24**, 953
- 3 Nguyen, H. X. and Ishida, H. *Am. Chem. Soc., Div. Polym. Chem. Polym. Prepr.* 1985, **26**, 273
- 4 Nguyen, H. X. and Ishida, H. *Polymer* 1986, **27**, 1400
- 5 Nguyen, H. X. *PhD Thesis* Case Western Reserve University, USA, 1986
- 6 Nguyen, H. X. and Ishida, H. *Makromol. Chem., Macromol. Symp.* 1986, **5**, 135
- 7 Voice, A. M., Bower, D. I. and Ward, I. M. *Polymer* 1993, **34**, 1154
- 8 Graf, R. T. *PhD Thesis* Case Western Reserve University, USA, 1985
- 9 Cunningham, A., Davies, G. R. and Ward, I. M. *Polymer* 1974, **15**, 743
- 10 Michele, A. and Vittoria, V. *Polym. Commun.* 1991, **32**, 232
- 11 Ohkoshi, Y., Ohshima, H., Matsuhisa, T., Toriumi, K. and Konda, A. *Sen-i Gakkaishi* 1990, **45**, 509
- 12 Ohkoshi, Y., Ohshima, H., Matsuhisa, T., Niyamoto, N., Toriumi, K. and Konda, A. *Sen-i Gakkaishi* 1990, **46**, 87
- 13 Lee, Y., Lefebvre, J. and Porter, R. S. *J. Polym. Sci., Polym. Phys. Edn* 1988, **26**, 795
- 14 Kunugi, T., Mizushima, A. and Hayakawa, T. *Polym. Commun.* 1986, **27**, 175
- 15 Rueda, D. R., Ania, F., Richardson, A., Ward, I. M. and Balta-Calleja, F. J. *Polym. Commun.* 1983, **24**, 258
- 16 Zhen, X. J., Kitao, T., Kimura, Y. and Taniguchi, I. *Sen-i Gakkaishi* 1985, **41**, T1